Radiological Dose Rate Calculations for the International Thermonuclear Experimental Reactor (ITER)

H.Y. Khater and R.T. Santoro

June 1996

UWFDM-1024

Presented at the 12th Topical Meeting on the Technology of Fusion Power, 16–20 June 1996, Reno NV.

FUSION TECHNOLOGY INSTITUTE

UNIVERSITY OF WISCONSIN

MADISON WISCONSIN

Radiological Dose Rate Calculations for the International Thermonuclear Experimental Reactor (ITER)

H.Y. Khater and R.T. Santoro

Fusion Technology Institute
University of Wisconsin
1500 Engineering Drive
Madison, WI 53706

http://fti.neep.wisc.edu

June 1996

UWFDM-1024

Presented at the 12th Topical Meeting on the Technology of Fusion Power, 16–20 June 1996, Reno NV.

RADIOLOGICAL DOSE RATE CALCULATIONS FOR THE INTERNATIONAL THERMONUCLEAR EXPERIMENTAL REACTOR (ITER)

H. Y. Khater
Fusion Technology Institute
University of Wisconsin-Madison
1500 Engineering Drive
Madison, WI 53706-1687
(608) 263-2167

R. T. Santoro
ITER JWS Garching Co-center
Boltzmannstrasse 2
D-85748 Garching
Germany

ABSTRACT

Two-dimensional biological dose rates were calculated at different locations outside the International Thermonuclear Experimental Reactor (ITER) design. An 18° sector of the reactor was modeled in r-ϑ geometry. The calculations were performed for three different pulsing scenarios. This included a single pulse of 1000 s duration, 10 pulses of 1000 s duration with a 50% duty factor, and 9470 pulses of 1000 s duration with a 50% duty factor for a total fluence of 0.3 MW·a/m^2. The dose rates were calculated as a function of toroidal angle at locations in the space between the toroidal field (TF) coils and cryostat, and in the space between the cryostat and the biological shield. The two-dimensional results clearly showed the toroidal effect, which is dominated by contribution from the activation of the cryostat and the biological shield. After one pulse, full access to the machine is possible within a few hours following shutdown. After 10 pulses, full access is also possible within the first day following shutdown. At the end of the Basic Performance Phase (BPP), full access is possible at any of the locations considered after one week following shutdown.

I. INTRODUCTION

Biological dose rate calculations were performed to assess the feasibility of performing maintenance on the International Thermonuclear Experimental Reactor (ITER). The current planning for ITER envisions two operational phases. The first phase is the Basic Performance Phase (BPP) which is supposed to last for ten years and involve a few thousand hours of D-T operation. The radioactivity induced in the reactor structure will depend on the pulsing scenarios that are being implemented during the BPP as well as the resulting neutron fluence. No tritium breeding is allowed during this phase. The BPP could be followed by an Enhanced Performance Phase (EPP), that lasts for another ten years and would emphasize improved performance and testing. The EPP envisions utilizing a tritium breeding blanket. The results presented in this paper deal only with the BPP and for the following pulse scenarios: one pulse of 1000 s duration, 10 pulses at 50% duty factor and continuous pulsing at 50% duty factor to accumulate a total fluence of 0.3 MW·a/m^2.

The latest ITER interim design[1] specifies a machine with the same overall dimensions as of earlier designs. In this paper we used a more detailed two-dimensional model than the one we used in our previous analysis[2] by adding the inter-coil structure, cryostat and biological shield. A simple schematic of the two-dimensional model showing locations at which dose rates were calculated is shown in Fig. 1. As shown in the figure, the radial build was modeled for a two-dimensional, r and ϑ ($-9° < \vartheta < 9°$) calculation.

II. CALCULATIONAL PROCEDURE

The spatial distribution of the neutron flux was calculated using the two-dimensional discrete ordinates neutron transport code TWODANT[3] together with 46 n-group and 21 g-group cross-sections that were collapsed from the fine group FENDL library. The analysis used a P_3 approximation for the scattering cross-sections and an S_8 angular quadrature set. The inboard and outboard regions were modeled simultaneously to account for toroidal effects and mutual neutron interactions between the two regions. The neutron flux was normalized to 1 MW/m^2 wall loading on the outboard side. A total of 8400 (525 $\times$ 16) mesh points were modeled. The activation analysis was performed using the DKR-ICF[4] code with cross section data from the USACT93[5] activation data base. The cross section library used contains data for 3000 nuclides. The gamma library contains data for 1788 nuclides and was taken from the ENDF/B-VI files. Gamma source from

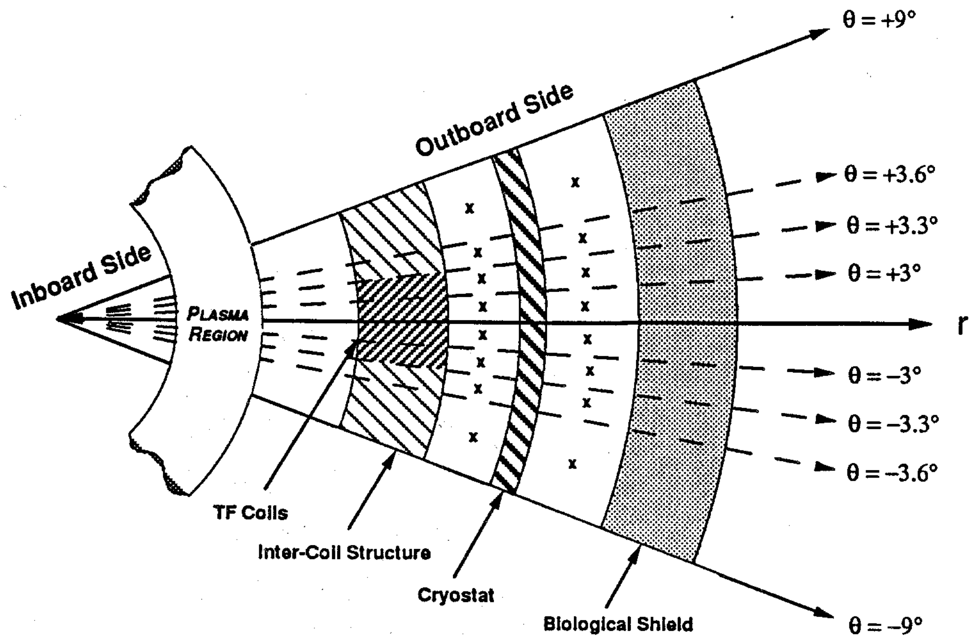

Fig. 1. Schematic of the two-dimensional r-ϑ model.

decay was determined at all mesh points and transported, using the TWODANT code, to calculate dose rate at different locations following shutdown. An inter-coil mechanical support was included in the space between the TF coils. The dose rates were calculated as a function of toroidal angle at locations shadowed by the magnet and in the space between magnets. In addition, a set of one-dimensional calculations was performed for the purpose of comparing their results to results obtained from the two-dimensional analysis.

The materials used in the activation analysis are a Cu-Be first wall, and water-cooled SS316-LN blanket and vacuum vessel. The TF coils consist of 18% epoxy insulator, 11.69% Cu conductor, 2.95% Nb_3Sn superconductor, 43.19% SS316-LN, 7.35% bronze, and 16.82% liquid helium. The cryostat is made of 100% SS316-LN and the biological shield consists of 98% concrete and 2% C1020 steel. The inter-coil mechanical support is made of SS316-LN and occupies 25% of the total volume between the TF coils. All impurities were included in the analysis.

III. BIOLOGICAL DOSE RATES

Dose rates were calculated as a function of toroidal angle at locations in the space between the TF coils and cryostat, and in the space between the cryostat and the biological shield. In addition, the dose rates were calculated at locations shadowed by the magnet and in the space between magnets. Figures 2 and 3 show the biological dose rates behind the TF coils and cryostat, and as functions of time following shutdown. A limit of 25 μSv/h for hands-on maintenance is used in this analysis assuming that the maintenance personnel work for 40 hours a week and 50 weeks a year. The dose rates for the first two scenarios exhibit a fairly rapid decay with increasing time after shutdown. After one pulse, full access to the machine

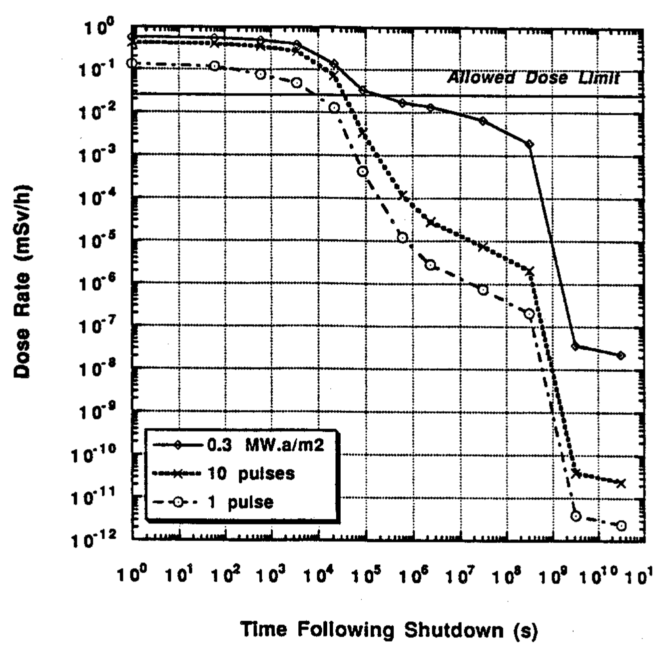

Fig. 2. Biological dose rates behind TF coils.

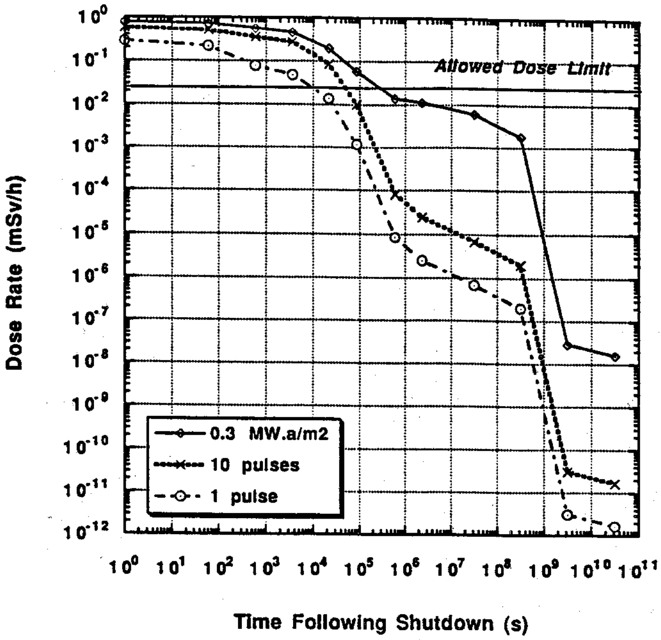

Fig. 3. Biological dose rates behind the cryostat.

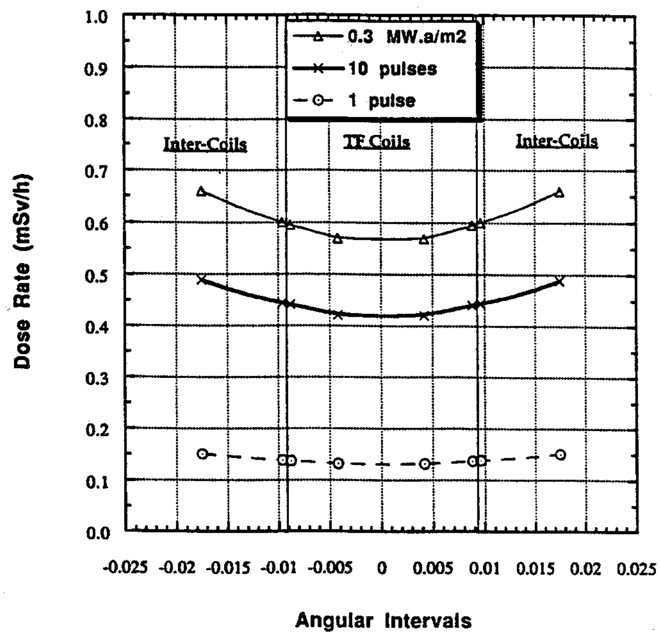

Fig. 4. Biological dose rates at shutdown behind TF coils as a function of angular intervals.

is possible within a few hours following shutdown. After 10 pulses, full access is also possible within the first day following shutdown. At the end of the Basic Performance Phase, full access is possible at any of the locations considered after one week following shutdown. For these operating conditions, personnel may enter the cryostat for quick maintenance tasks assuming that the nearby penetrations are sufficiently shielded so that dose from local hot spots is small.

As shown in Figs. 4 and 5, the two-dimensional results clearly showed the toroidal effect which is dominated by contribution from the activation of the cryostat and the biological shield. Adding the inter-coil mechanical support provided more shielding behind the vacuum vessel resulting in a reduction of the biological dose rate (1 day following shutdown) by a factor of five when compared to previous[2] two-dimensional calculations that did not include the inter-coil structure.

A set of one-dimensional calculations was also performed for comparison with the two-dimensional analysis. As shown in Table I, a comparison between the one-dimensional (1-D) and two-dimensional (2-D) results showed that, at one day after shutdown, the one-dimensional calculation significantly underestimates the biological dose rates behind the TF coils. On the other hand, the one-dimensional results are about 50% higher than the two-dimensional results in areas shadowed by the inter-coil structure (between coils). Results in Table I also showed that ^{24}Na produced in the concrete part of the

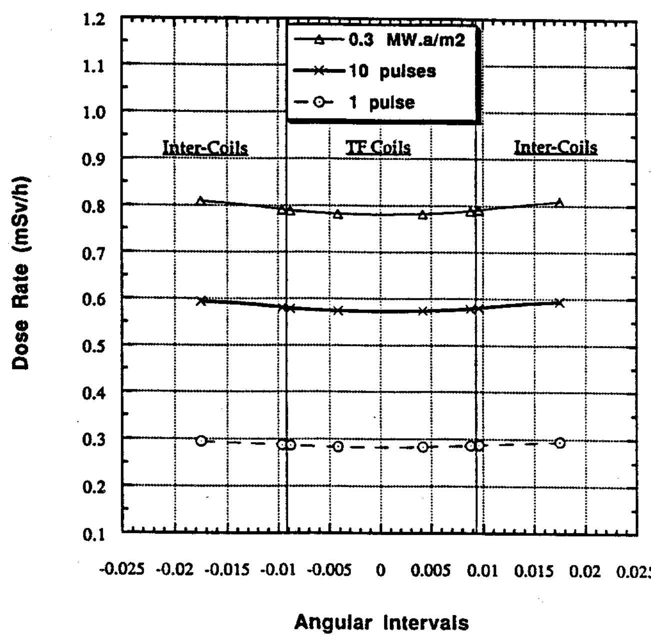

Fig. 5. Biological dose rates at shutdown behind cryostat as a function of angular intervals.

biological shield is the major contributor to the dose. The level of contribution is given between parentheses.

In order to reduce the ^{24}Na dose, we examined the possibility of adding a 1 cm-thick layer of boron to the front of the concrete biological shield. As shown in

TABLE I

Biological Dose Rates After One Day Following Shutdown Using 2-D and 1-D Models

Model	Location	Dose (mSv/hr)	Dominant Nuclides	Source of Nuclides
2-D	between coils and cryostat (coils shadow)	0.0337	(1) ^{24}Na (29%)	bio-shield (100%)
			(2) ^{60}Co (21%)	cryostat (53%) inter-coils (24%) TFC (17%)
1-D	between coils and cryostat (coils shadow)	1.53e-7	(1) ^{24}Na (23%)	bio-shield (100%)
			(2) ^{60}Co (21%)	TFC (52%) cryostat (43%)
			(3) ^{99}Mo (21%)	TFC (56%) cryostat (44%)
2-D	between coils and cryostat	0.0395	(1) ^{24}Na (25%)	bio-shield (100%)
			(2) ^{60}Co (21%)	cryostat (45%) inter-coils (45%) TFC (5%)
			(3) ^{58}Co (15%)	inter-coils (69%) cryostat (30%)
1-D	between coils and cryostat	0.0555	(1) ^{24}Na (27%)	bio-shield (100%)
			(2) ^{60}Co (22%)	cryostat (49%) inter-coils (46%)
			(3) ^{99}Mo (15%)	inter-coils (52%) cryostat (47%)
2-D	between cryostat and bio-shield (coils shadow)	0.0586	(1) ^{24}Na (69%)	bio-shield (100%)
			(2) ^{60}Co (11%)	cryostat (63%) bio-shield (29%)
1-D	between cryostat and bio-shield (coils shadow)	2.3e-7	(1) ^{24}Na (65%)	bio-shield (100%)
			(2) ^{60}Co (12%)	cryostat (62%) bio-shield (27%) TFC (10%)
2-D	between cryostat and bio-shield	0.0608	(1) ^{24}Na (68%)	bio-shield (100%)
			(2) ^{60}Co (11%)	cryostat (63%) bio-shield (29%)
1-D	between cryostat and bio-shield	0.0928	(1) ^{24}Na (69%)	bio-shield (100%)
			(2) ^{60}Co (12%)	cryostat (63%) bio-shield (29%) inter-coils (8%)
			(3) ^{59}Fe (6%)	cryostat (65%) bio-shield (27%) inter-coils (8%)

Table II, adding the 1 cm boron layer reduced the dose at locations between the coils and cryostat by 65% due to reduction in thermal neutron capture in the concrete. Adding the boron layer resulted in the reduction of the dose between the cryostat and biological shield by a factor of three.

IV. SUMMARY

A detailed two-dimensional activation analysis was performed to calculate biological dose rates at different locations outside the International Thermonuclear Experimental Reactor (ITER) design. An 18° sector of the

Table II

The Impact of Adding a Layer of Boron to the Biological Shield

Model	Location	Dose (mSv/hr)	Dominant Nuclides	Source of Nuclides
2-D (without boron)	between coils and cryostat	0.0395	(1) ^{24}Na (25%)	bio-shield (100%)
			(2) ^{60}Co (21%)	cryostat (45%) inter-coils (45%) TFC (5%)
			(3) ^{58}Co (15%)	inter-coils (69%) cryostat (30%)
2-D (with boron)	between coils and cryostat	0.0259	(1) ^{58}Co (22%)	inter-coils (69%) TFC (11%)
			(2) ^{60}Co (19%)	inter-coils (62%) cryostat (30%)
			(3) ^{99}Mo (18%)	inter-coils (57%) cryostat (37%)
2-D (without boron)	between cryostat and bio-shield	0.0608	(1) ^{24}Na (68%)	bio-shield (100%)
			(2) ^{60}Co (11%)	cryostat (63%) bio-shield (29%)
2-D (with boron)	between cryostat and bio-shield	0.0197	(1) ^{24}Na (63%)	bio-shield (100%)
			(2) ^{60}Co (9%)	cryostat (45%) bio-shield (30%

reactor was modeled in a two-dimensional r-ϑ geometry. The calculation was performed for one pulse of 1000 s duration, 10 pulses at 50% duty factor and continuous pulsing at 50% duty factor to accumulate a total fluence of 0.3 MW·a/m^2. The dose rates were calculated as a function of toroidal angle at locations in the space between the TF coils and cryostat, and in the space between the cryostat and the biological shield. The dose rates for the first two scenarios exhibit a fairly rapid decay with increasing time after shutdown. At the end of the Basic Performance Phase, full access is possible at any of the locations considered after one week following shutdown. Adding a 1 cm-thick layer of boron to the front of the concrete biological shield reduces the dose at locations between the coils and cryostat by 65% and reduces the dose between the cryostat and biological shield by a factor of three. A further analysis to include effects of streaming through ducts will be starting in the near future.

ACKNOWLEDGMENT

This report is an account of work performed under the agreement among the European Atomic Energy Community, the Government of Japan, the Government of the Russian Federation, and the Government of the United States of America on Cooperation in the Engineering Design Activities for the International Thermonuclear Experimental Reactor ("ITER EDA Agreement") under the auspices of the International Atomic Agency (IAEA).

REFERENCES

1. Technical Basis for the ITER Interim Design Report, Cost Review and Safety Analysis, ITER EDA Documentation Series, No. 7, International Atomic Energy Agency, Vienna, April 1996.
2. R. T. Santoro, et al., "Nuclear Analysis in Support of ITER Design," Proceedings of the 16th IEEE/NPPS Symposium on Fusion Engineering, October 1-5, 1995, Champaign, IL.
3. R. Alcouffe et al., User's Guide for TWODANT: A Code Package for Two-Dimensional, Diffusion-Accelerated, Neutral-Particle Transport, Los Alamos National Laboratory, LA-10049-M (March 1984).
4. D. L. Henderson and O. Yasar, "DKR-ICF: A Radio-activity and Dose Rate Calculation Code Package," UWFDM-714, Vol. 1, University of Wisconsin (April 1987).
5. F. M. Mann and D. E. Lessor, "REAC*3 Nuclear Data Libraries," Proceedings of an International Conference, Nuclear Data for Science and Technology, May 1991, Jülich, Federal Republic of Germany, S. Qaim (ed.), Springer-Verlag, p. 936.